FIELD PERFORMANCE OF A HYBRID REINFORCED EARTH EMBANKMENT BUILT ADJACENT TO A SLOPE WITH NARROW FILL SPACE

Chia-Cheng Fan[1] and Chin-Fu Hsiao[2]

ABSTRACT

This paper presents a field monitoring results on the performance of a hybrid reinforced earth embankment, used for mountain roadway, built adjacent to a slope with narrow fill space. The hybrid reinforced earth embankment incorporates reinforced earth embankments with soil nails which are installed to the existing ground. To investigate the effectiveness of soil nails connected at back of a reinforced earth embankment, a field monitoring program on reinforcement stresses and nail forces in the hybrid reinforced earth embankment was set up for an 8-m-high earth embankment. The performance of the embankment during construction and under various loadings, including static and traffic loadings, was investigated and discussed.

Key words: Reinforced earth embankment, soil nails, full-scale tests, traffic loading, static loading.

1. INTRODUCTION

Reinforced earth retaining structures are conventionally used in areas where the fill space is sufficiently wide for placing reinforcements with required lengths. Methods for analyzing the safety of reinforced earth retaining structures have been well developed and established during the past decades (Elias *et al* 2001). Reinforced earth embankments are being used increasingly in transportation projects throughout the world. In mountainous region, however, building a stable reinforced earth embankment may be somewhat difficult due to steep slopes or insufficient fill spaces for placing reinforcements.

A hybrid reinforced earth embankment system was developed by Fan and Hsieh (2007) to use in area where the fill space is restricted. The hybrid reinforced earth system incorporates a reinforced earth embankment with soil nails which are installed to the existing ground, as shown in Fig. 1(a). Soil nails provide additional resisting forces to stabilize the reinforced earth embankment which is potentially unstable due to insufficient reinforcement lengths. Additionally, flexible connecting elements (system), as shown in Fig. 1(b), were developed to tie the reinforcements within reinforced earth embankments to soil nails installed in the existing ground behind the embankment. The existing ground is considered a firm geological material. The connecting structure, improved from a patented connecting method (Chou and Fan 2004), consisting of a series of stainless steel wire ropes and stainless steel pipes on the existing slope.

The behavior of reinforced earth structures has been well known through experimental studies (Simac *et al.* 1990; Allen *et al.* 1992; Fishman *et al.* 1993; Bathurst *et al*. 2000; Bathurst *et al.* 2003) and numerical modeling (Karpurapu and Bathurst 1995). Nevertheless, the behavior of the hybrid reinforced earth embankment shown in Fig. 1 has not been studied in experimental works. To enhance the future use of the hybrid reinforced earth embankment in engineering practices, the mechanical behavior of the embankment system needs to be further investigated.

This paper aims to present a field monitoring results on the performance of a hybrid reinforced earth embankment, as proposed in Fig. 1, built adjacent to a slope with limited fill space. Soil nails in firm existing ground bear the driving force induced during the construction of the embankment to some extent. To investigate the effectiveness of soil nails connected at back of a reinforced earth embankment, a field monitoring program on reinforcement stresses and nail forces induced during the construction of the embankment and under various loading conditions, including static and traffic loadings, was set up for an 8-m-high hybrid reinforced earth embankment. A 12-ton vehicle driving at uphill and downhill conditions was carried out. In addition, the impact of emergency brake of moving vehicles on the stress distribution of reinforcing materials was also studied.

2. MATERIALS AND METHODS

2.1 Experimental Site

The site of the research project is located at Liouguei in Kaohsiung city, Taiwan, as shown in Fig. 2. The project site is about 1.5 km north of downtown of Liouguei. The width of the mountain roadway is 4 ~ 5 m. The slope gradients of the upslope and downslope of the roadway are about 30° ~ 50° and 25° ~ 40°, respectively. This roadway collapsed in the summer of 2005 due to the attack of several Typhoons. The retaining structure supporting the roadway embankment prior to the collapse was reinforced concrete retaining walls. The length of the collapse roadway was about 100 m. The photos of the collapsed roadway are shown in Fig. 3. The roadway runs across a gullied slope. This location was severely damaged due to the heavy rainfall in 2005. The embankment of the collapsed mountain roadway was located on a concave section. The surface runoff collected in the concave section imposed a high water pressure on the back of the wall and

Manuscript received September 30, 2010; revised March 17, 2011; accepted March 18, 2011.

[1] Associate professor (corresponding author), Dept. of Construction Engineering, National Kaohsiung First University of Science and Technology, Kaohsiung, Taiwan (e-mail: ccfan@ccms.nkfust.edu.tw).

[2] Former graduate student, Dept. of Construction Engineering, National Kaohsiung First University of Science and Technology, Kaohsiung, Taiwan.

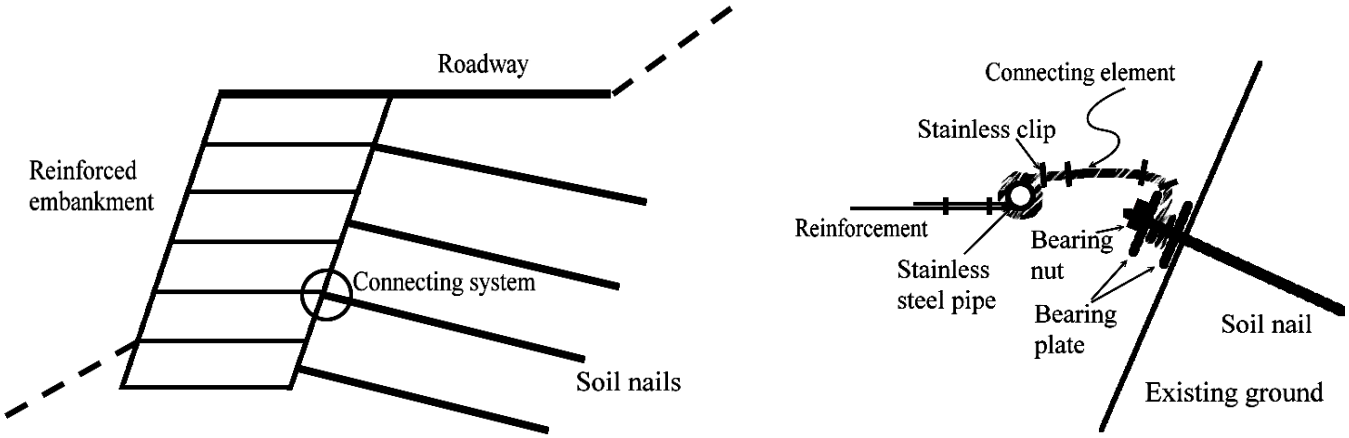

(a) A hybrid embankment system (b) Details of connecting elements

Fig. 1 Illustration of a hybrid reinforced embankment system used as the embankment of roadways in mountainous area (Fan and Hsieh 2007)

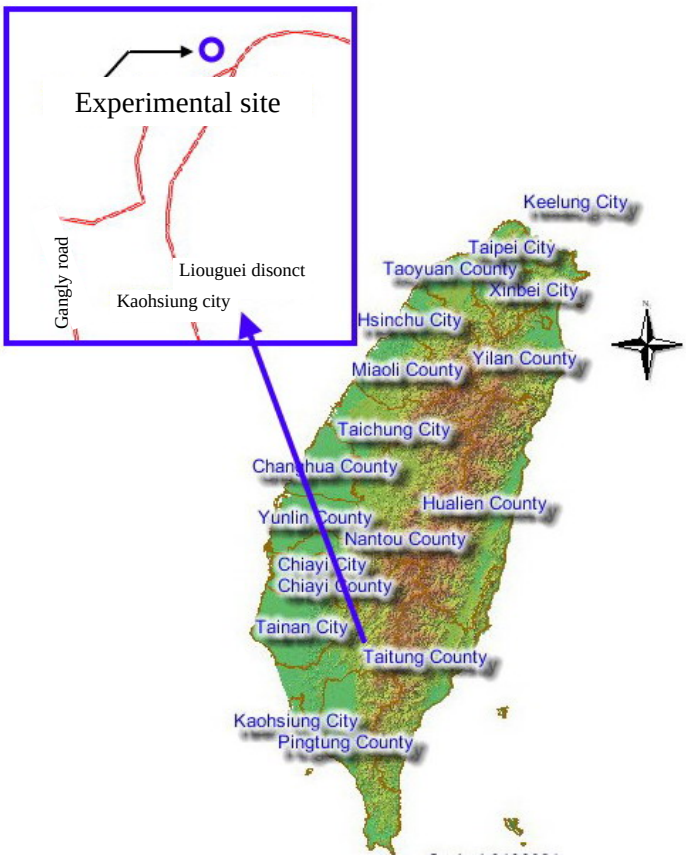

Fig. 2 Location of the experimental site (The map was from the web site of the Ministry of the Interior, Taiwan)

(a)

(b)

Fig. 3 Collapse of a mountainous roadway at Liouguei, Kaohsiung City, Taiwan

softened the backfill material. In addition, the downslope of the embankment was steep and subject to erosion in rainy season. The poor drainage system in the retaining wall was regarded as the major reason blamed for the failure of the roadway embankment.

2.2 Construction of Geosynthetic Reinforced Earth Embankment

The collapsed roadway was rehabilitated using reinforced earth embankments. However, the roadway width for some part of the roadway is not sufficient to place reinforcing materials with satisfactory length to ensure the stability of the embankment. Thus, the hybrid reinforced earth embankment system as shown in Fig. 1 was used for some part of the roadway. The hybrid reinforced earth system incorporates a reinforced earth embankment with soil nails which are installed to the existing ground, as shown in Fig. 1(a). Layout of the roadway rehabilitated using reinforced earth embankments is shown in Fig. 4.

Extensible PET geogrids with tensile strength of 150 kN × 75 kN (Seven-state Inc.) were used for the reinforcing material, and soil nails used were #10 rebar (32 mm in diameter) surrounded by 10 cm diameter ring of cement mortar. Stainless steel wire ropes, connecting elements, were used to connect soil nails and reinforcing materials by binding the nail's head and the steel pipe. At least a pair of stainless steel wire rope clips is used to tie the stainless steel wire rope at both ends. The diameter of the Stainless steel wire rope was about 0.016 m. The backfill material consisted mainly of silty materials mixed with sands. The degree of compaction for the backfilling was required to be greater than 90%. Typical design cross-section of the hybrid reinforced earth embankment is shown in Fig. 5. Construction of the hybrid reinforced earth embankment is demonstrated in Fig. 6. The slope adjacent to the roadway embankment was excavated and trimmed before soil nails can be installed, followed by the construction of the reinforced earth embankment. Figure 7 shows the completed embankment at the experimental site.

2.3 Instrumentations

The instrumentations of the hybrid reinforced earth embankment are shown in Fig. 5. The embankment height and roadway width were 8 m and 6 m, respectively, and the slope gradient of the embankment facing was 75°. Seventeen layers of reinforcing materials were installed in the embankment. The vertical spacing of the reinforcing materials was 0.5 m. The reinforcement length from the top to a depth of 1.5 m was 5.7 m, and it was 5 m below the depth of 1.5 m. Nail length and vertical spacing of soil nails were 4 m and 1 m, respectively.

Sixty-four strain gages were placed on reinforcing materials at depths of 6.5 m, 5.5 m, 4.5 m, 3.5 m, 2.5 m, 2 m, 1.5 m, 1 m, and 0.5 m, and thirty-six strain gages were placed on soil nails at depths of 5.5 m, 4.5 m, 3.5 m, 2.5 m, 1.5 m, and 0.5 m. KYOWA strain gages (product number: KFP-5-120-C1-65L5M2R), which are good for plastic materials, were used for the reinforcing materials (geogrids), and strain gages (product number: KFG-5-120-C1-11L5M2R) were used for metal materials (soil nails). The strain gages were protected from rainfall-induced infiltration by using water-proof cement. All the installation of strain gages were carried out in the laboratory.

Strains developed in reinforcing materials and soil nails during the construction were monitored, and strains were transformed to forces. The stress distribution in the hybrid reinforced earth embankment during and following the construction can be obtained through the instrumentation project.

Soil nails were installed in the existing slope prior to the construction of the roadway embankment. The embankment was built according to standard construction procedure in the field. The reinforcement stresses monitored can represent the field performance of the reinforced earth embankment. The stress distribution of reinforcement and soil nails in the embankment was investigated under uniform static loading of 8 kPa, 12 kPa, and 20 kPa. In addition, vehicles driving at uphill and downhill conditions were also carried out.

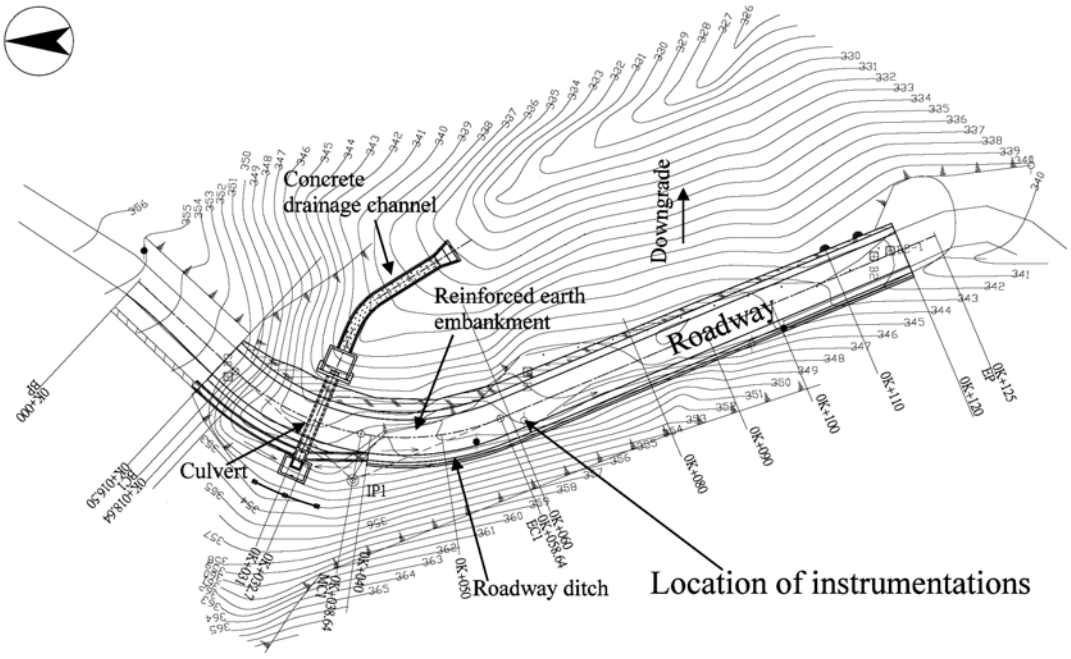

Fig. 4 Layout of the mountain roadway rebuilt with the hybrid reinforced earth embankment

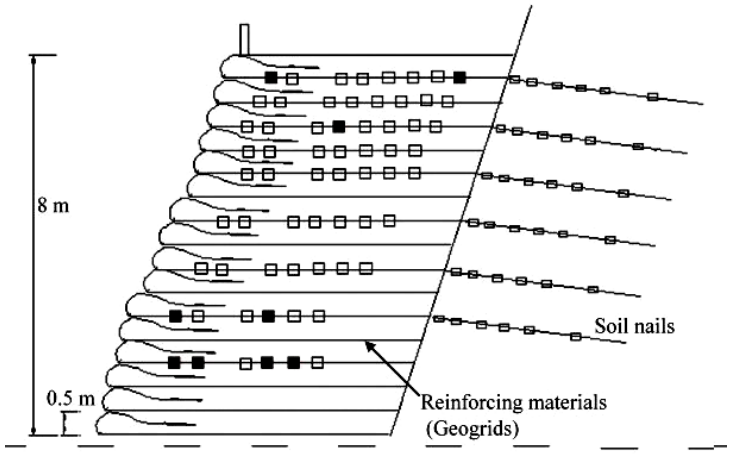

Fig. 5 Typical design cross-section and instrumentation of the hybrid reinforced earth embankment (Note: strain gages are marked with hollow square, and the strain gages with dark square were destroyed after the construction of the embankment)

(a) Building embankment facing

(b) Backfilling

(c) Installation of reinforcement placed with strain gages

(d) Compaction

Fig. 6 Construction of the hybrid reinforced earth embankment at the experimental site

Fig. 7 The completed embankment at the experimental site and subjected to traffic loading

2.4 Tensile Forces of Reinforcements

Strains developed in geogrids and soil nails during the construction and under various loading conditions were transformed into forces. The tensile modulus of the geogrid was 1,215 kN/m based on the tensile test results. The elastic modulus in tensile mode and cross-sectional area for soil nails were 2.04×10^8 kPa and 8.55 cm^2, respectively. The forces developed in geogrids and soil nails can be computed as

$$T_g = K_s \cdot \varepsilon_g \quad (1)$$

$$T_r = (E_r\ A) \cdot \varepsilon_r \quad (2)$$

where T_g (kN/m) and T_r (kN) are reinforcement stresses and nail forces, respectively; ε_g and ε_r are strains developed in geogrids and soil nails, respectively; K_s is the tensile modulus of geogrids; E_r and A are the elastic modulus and cross-sectional area of soil nails, respectively.

3. RESULTS AND DISCUSSION

3.1 Stress Distribution of Reinforcements during Construction

Figure 8 shows the monitored distribution of reinforcement (geogrid) stresses at depths of 5.5 m, 4.5 m, 3.5 m, 2.5 m, 2 m, 1.5 m, and 1 m below the top of the embankment during the construction. Most of the reinforcement stresses were developed at about 2 ~ 4 m from the edge of the roadway. The reinforcement stresses were mobilized partly due to the weight of the fill, in addition, the construction loads induced by trucks, backhoes, and smooth-wheel rollers also contribute considerably to the mobilization of reinforcement stresses.

The maximum reinforcement stresses at various elevations following the construction reach to about 2 ~ 4 kN/m, and the maximum reinforcement stresses occurs at about 1/2 to 2/3 reinforcement length away from the edge of the roadway. The maximum reinforcement stress following the construction of the embankment reaches to about 4 kN/m and takes place at a depth of 4.5 m below the top of the embankment, and this reinforcement stress corresponds to a tensile strain of about 0.33%. Field measurements on reinforced earth walls (Simac *et al*. 1990; Allen *et al*. 1992) showed that reinforcement strains were in the range of 0.1% to 0.5%, and most of the strains occurred during the construction stage. These observed results are close to those obtained in the research.

In addition, distribution of the tensile forces along the depth developed in soil nails at depths of 5.5 m, 4.5 m, 3.5 m, 2.5 m, 1.5 m, and 1 m below the top of the embankment during the construction is also shown in Fig. 8. The maximum nail force at different elevations during the construction is mobilized at the head, and the tensile forces fade away along the length of the nail. The mobilized nail forces comply with the mechanism of the stress distribution of the embankment system, *i.e.* soil nails provide extra resisting forces which the reinforced earth embankment needs to reach a safe condition. The nail forces at the depth less than 2 m are minor, and the maximum nail force reaches to about 22 kN. The maximum nail force along the depth takes place at a depth of 4.5m, and the value is 160 kN.

Figure 9 shows the stress distribution of reinforcing materials (geogrids) and soil nails in the hybrid reinforced earth embankment following the construction. The mechanism of stress transfer from reinforcement to soil nails can be clearly identified in this plot. The front end of the nails (nail's head) transmits the stress developed in the reinforcements within the embankment during and following the construction. Most of the reinforcement stresses and nail forces are mobilized during the construction stage. The maximum reinforcement stress and the maximum nail force developed following the construction occurred at a depth of 4.5 m below the top surface of the embankment. The maximum nail force at various elevations occurred at the nail head. Additionally, the tensile forces in soil nails dissipate along its length.

The monitored data demonstrate that reinforcement stresses following the construction of the embankment are considerably small compared with the ultimate tensile strength of geogrids normally used in engineering practice, and the maximum strain level of the reinforcement which may develop following the construction is also low. Use of reinforcements (geogrids) with high tensile strength in the design of geosynthetic reinforced earth structures may not be necessary based on the research results obtained herein. In addition, the stress transfer from reinforcements to soil nails can be verified through the monitored data, and it is useful to enhance the application of the hybrid reinforced earth embankment to other similar engineering projects.

3.2 Stress Distribution of Reinforcements under Static Loading

Static loads of 8 kPa, 12 kPa, and 20 kPa, induced by 8-ton, 12-ton, and 20-ton backhoe on a 10 m^2 metal plate with a thickness of 0.15 m, were applied on the top of the embankment roadway following the construction of the embankment. The monitored strains in reinforcements and soil nails were transformed into stresses and forces, respectively. Figure 10 shows the distribution of reinforcement (geogrid) stress increment and nail force increment at depths of 5.5 m, 4.5 m, 3.5 m, 2.5 m, 2 m, 1.5 m, and 1 m below the top of the embankment under static loading. The static loading has a considerable influence on the reinforcement stress increment at a depth less than 1.5 m. The maximum reinforcement stress increment was 0.3 kN/m for the reinforcement at a depth of 1 m, corresponding to a strain increment of 0.026%. The maximum reinforcement stress induced at a depth of 1 m following the construction of the embankment was 3.6 kN/m, corresponding to a strain of about 0.3%. The 20-kPa static loading on the roadway results in an increase of 8.3% in the reinforcement stress with respect to that following the construction.

Additionally, distribution of the tensile force increment mobilized in soil nails along the length at depths of 5.5 m, 4.5 m, 3.5 m, 2.5 m, and 1.5 m below the top of the embankment under static loading is shown in Fig. 10. The maximum increment in the nail force increases with the depth, and it ranges from 12 kN to 30 kN. The reinforcement stress increment and nail force increment increases with the quantity of the loading at various depths.

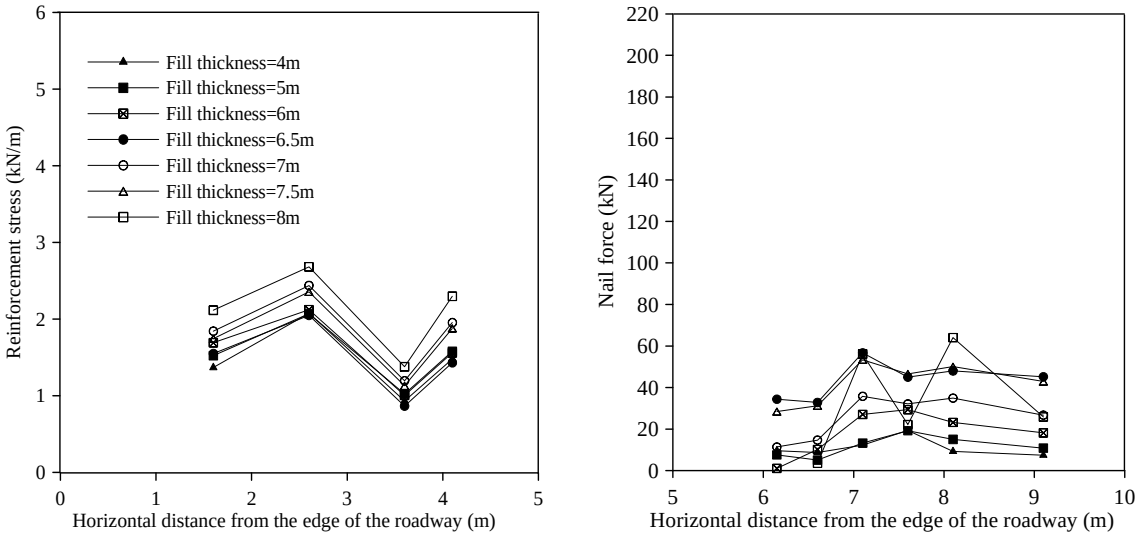

(a) depth = 5.5 m

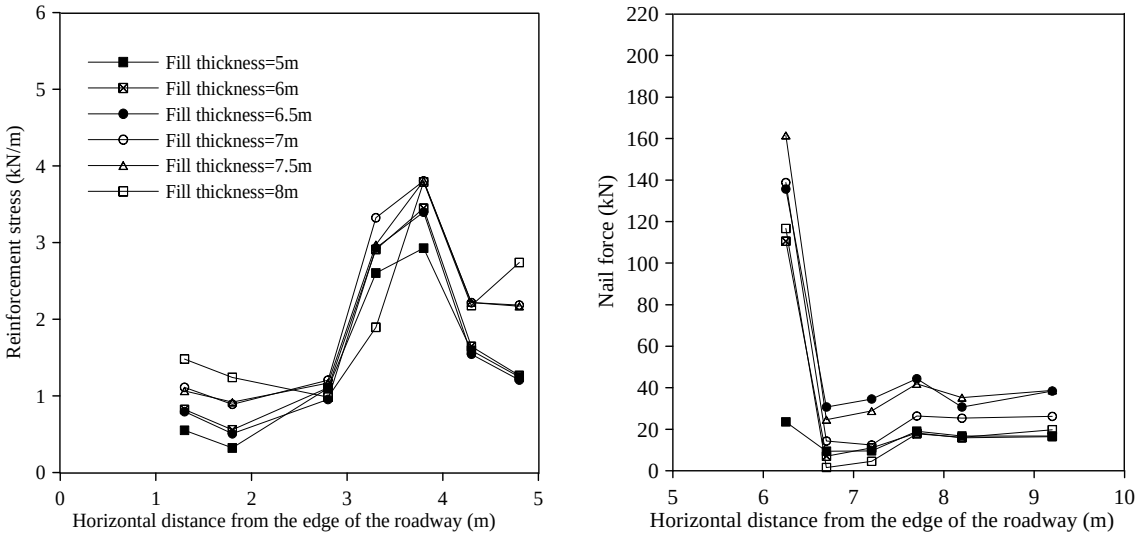

(b) depth = 4.5 m

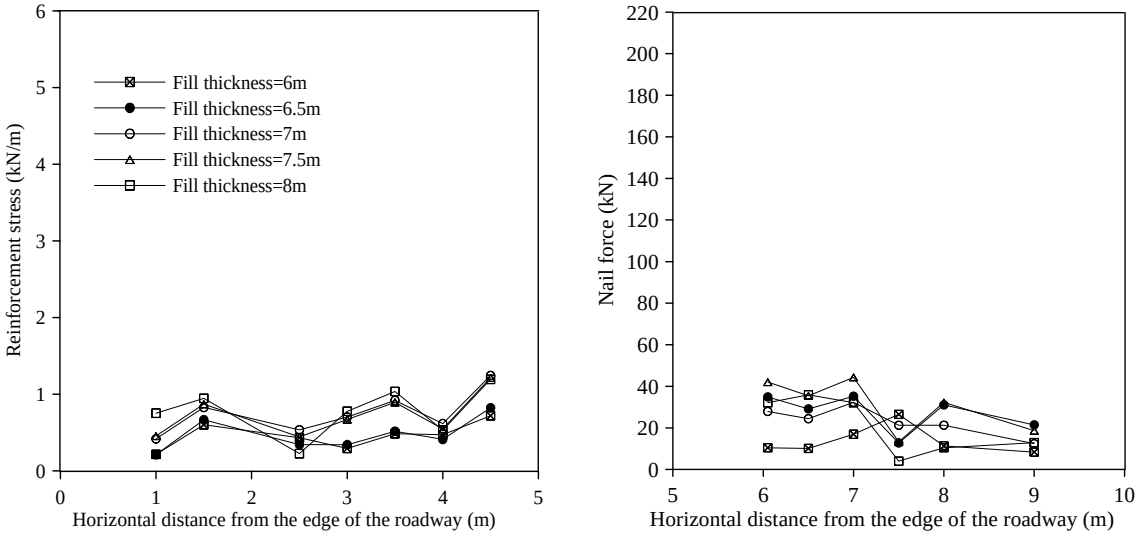

(c) depth = 3.5 m

Fig. 8 Distribution of reinforcement (geogrid) stresses and nail forces of the embankment during the construction

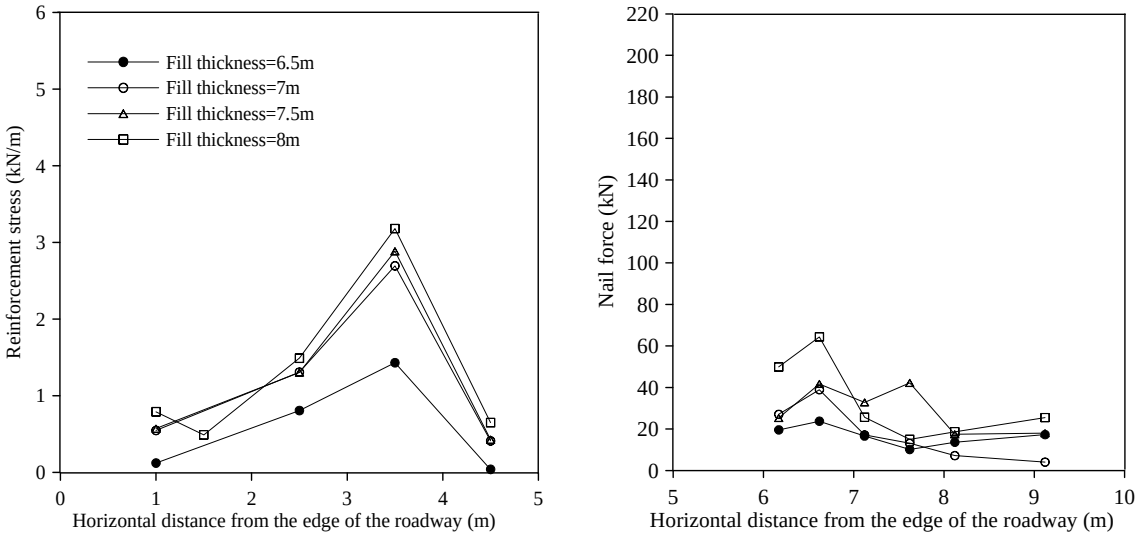

(d) depth = 2.5 m

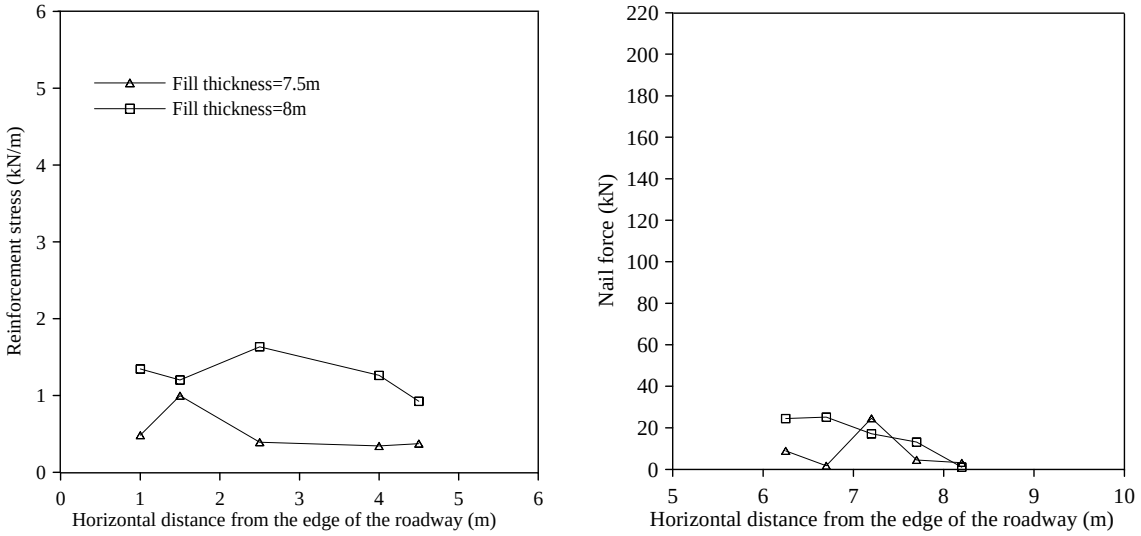

(e) depth = 1.5 m

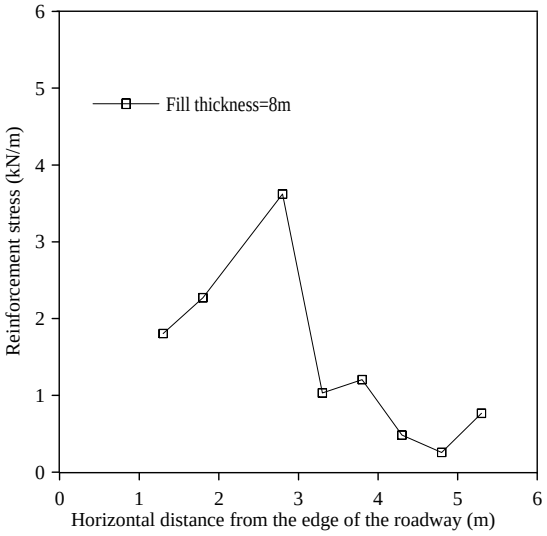

(f) depth = 1 m

Fig. 8 Distribution of reinforcement (geogrid) stresses and nail forces of the embankment during the construction (continued)

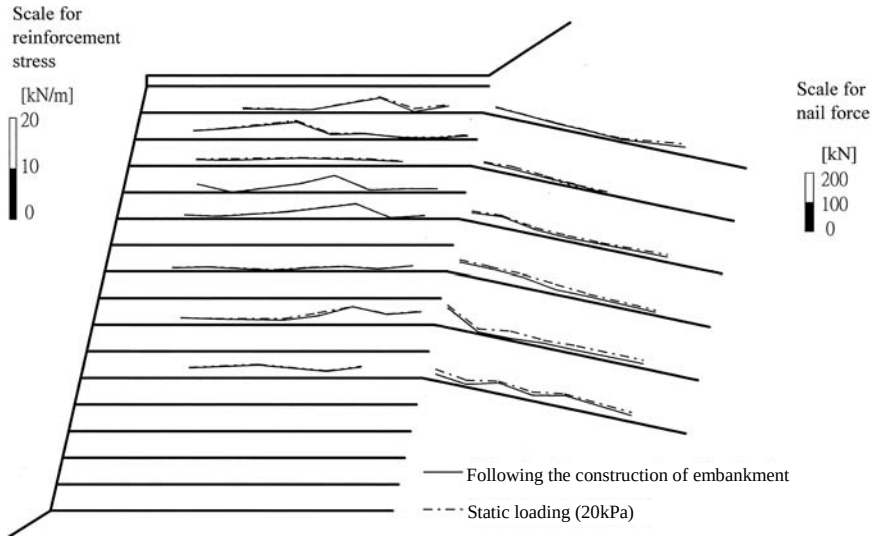

Fig. 9 Stress distribution of reinforcing materials (geogrids) and soil nails in the hybrid reinforced earth embankment following the construction and under 20 kPa static loading

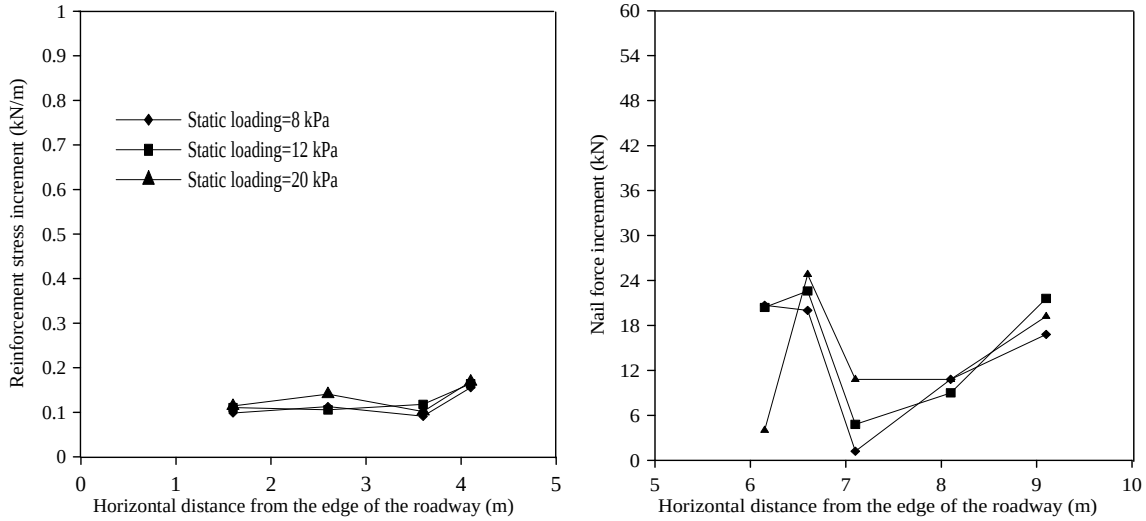

(a) depth = 5.5m

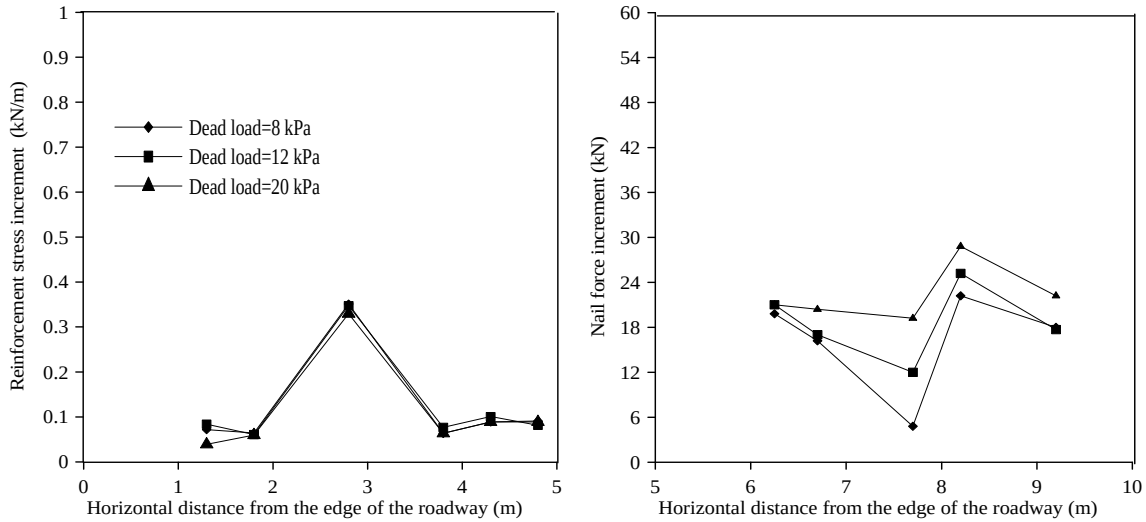

(b) depth = 4.5m

Fig. 10 Distribution of reinforcement (geogrid) stress increment and nail force increment of the embankment under static loading

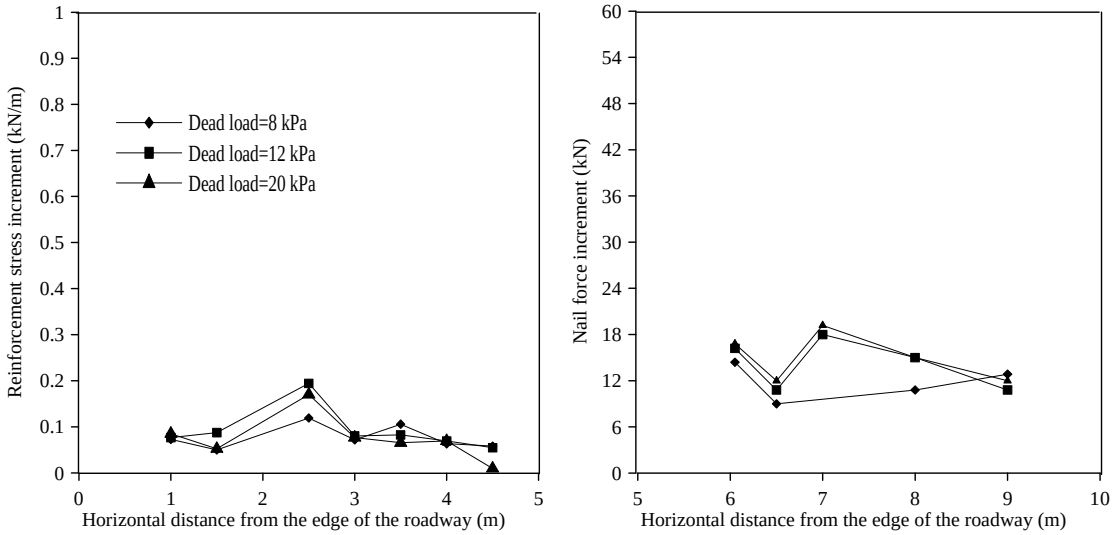

(c) depth = 3.5m

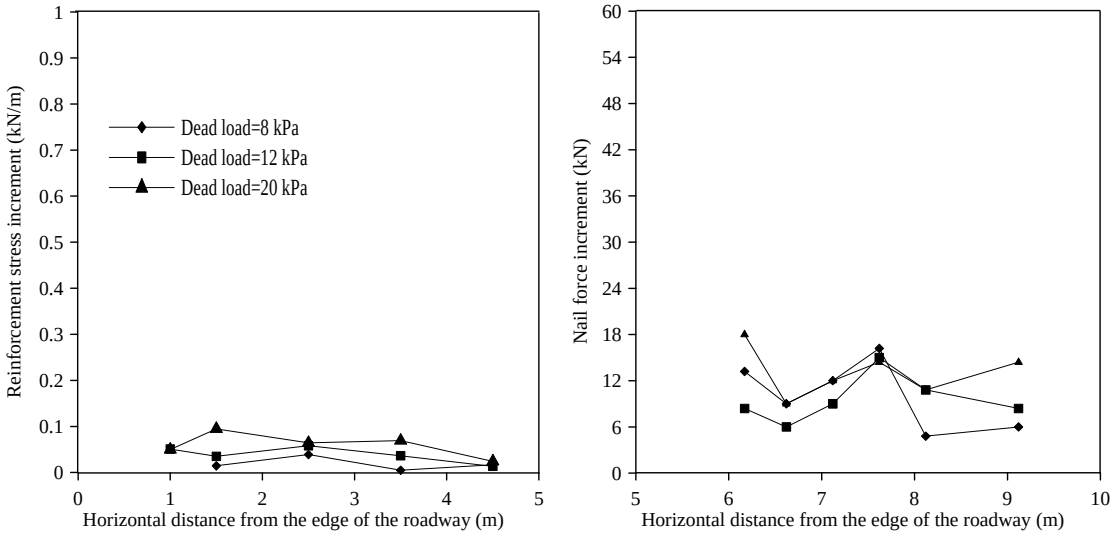

(d) depth = 2.5m

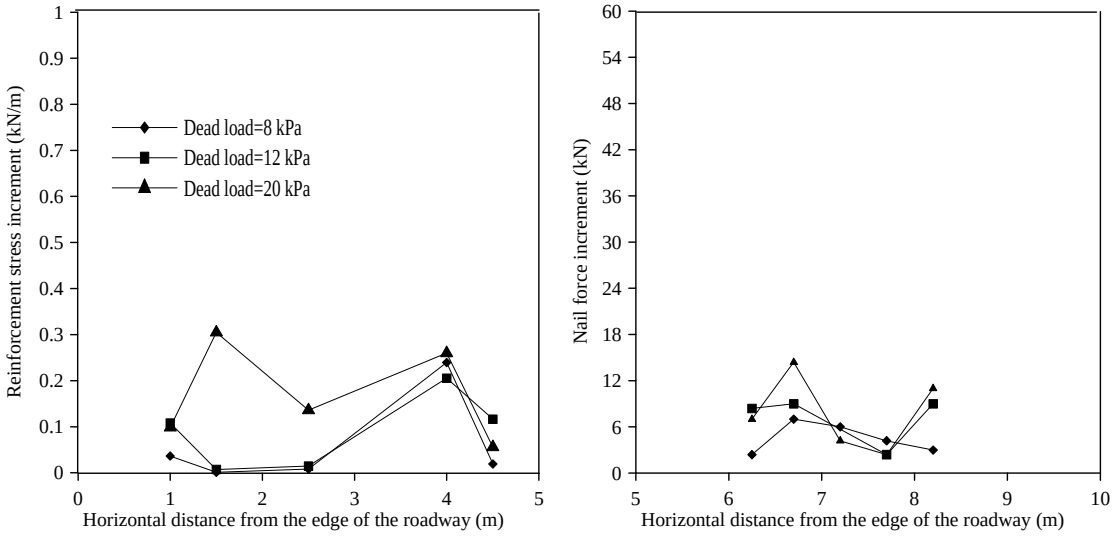

(e) depth = 1.5m

Fig. 10 Distribution of reinforcement (geogrid) stress increment and nail force increment of the embankment under static loading (continued)

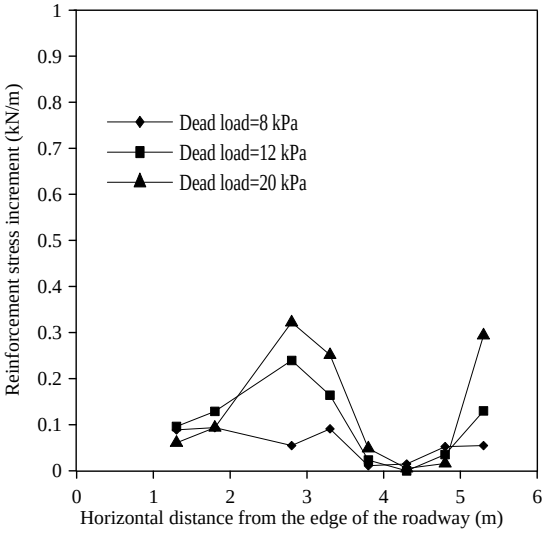

(f) depth = 1m

Fig. 10 Distribution of reinforcement (geogrid) stress increment and nail force increment of the embankment under static loading (continued)

3.3 Stress Distribution of Reinforcements under Traffic Loading

The vehicle speeds used for traffic loading were 10 km/hr, 20 km/hr and 30 km/hr. Because of close proximity of a curved section at the test site and a 10% gradient on the roadway, the test on the traffic loading with speed of 30 km/hr was thus unable to conduct due to safety consideration. This study only discusses on the results with vehicle speed of 10 km/hr and 20 km/hr.

Shown in Fig. 11 is the monitoring result of tensile stress increment on the 12-ton concrete mixer truck driving through uphill and downhill conditions at a speed of 10 km/hr and 20 km/hr. The results at a depth of 4.5 m, 3.5 m, 2.5 m, 2 m, 1.5 m, 1 m and 0.5 m from the road surface are presented.

The test results show that there is no significant impact on driving speed towards reinforcement stress increment. The tensile stress increment on reinforcements decreases with increasing depth. The reinforcement within 1 m below the road surface developed a greater tensile stress increment compared with that at depth below 1 m. At downhill conditions, the maximum stress increment on the reinforcement at 0.5 m below the road surface occurred at the end section of the reinforcement with a value of about 0.18 kN/m, while the maximum stress increment on the reinforcement at 1 m below the road surface occurred at the central portion of reinforcement with a value of about 0.14 kN/m. The maximum stress increment on reinforcements within 1 m below the road surface is about 0.4 ~ 0.6 kN/m for the embankment under 20-kPa static loading. The tensile stress increment on reinforcement caused by traffic loading of the 12-ton concrete mixer truck is about 30% of that induced by 20-kPa static loading. The maximum force increment on soil nails in various depths caused by the 12-ton vehicle driving through downhill conditions falls roughly within 0.48 ~ 1.44 kN.

In addition, at uphill conditions, the maximum tensile stress increment on the reinforcement at 0.5 m below the road surface occurred at the end section of reinforcement with a value of about 0.15 kN/m, while the maximum tensile stress increment on the reinforcement at 1.0 m below the road surface occurred at the central portion of the reinforcement with a value of about 0.14 kN/m. The tensile stress increment on the reinforcement caused by the 12-ton vehicle driving through uphill conditions is about 25% ~ 30% of that induced by 20-kPa static loading. In addition, the results under uphill and downhill driving conditions of the 12-ton vehicle have no significant variance towards the tensile stress increment on reinforcements.

The maximum force increments on soil nails at a depth of 0.5 m and 1.5 m are about 0.5 kN and 1.2 kN, respectively. The maximum forces on soil nails at a depth of 1.5 m and 4.5 m below the road surface following completion of reinforced earth embankment are 22 kN and 160 kN, respectively. The maximum force increment on soil nails caused by the 12-ton vehicle driving through uphill conditions is remarkably lower than the tensile force developed following the construction of the embankment. The maximum force increment on soil nails at 1.5 m below the road surface caused by the 12-ton vehicle is about 5% of that developed following the construction of the embankment. In addition, effect of driving at uphill and downhill conditions on the force increment of soil nails developed is not noticeable.

3.4 Stress Distribution of Reinforcements under Emergency Brake of Moving Vehicles

Emergency brake of moving vehicles results in a negative acceleration on the road surface. Thus, higher load amplitude on the roadway under emergency brake of moving vehicles can be expected in comparison with that caused by vehicles driving at a constant speed. Comparison of the stress/force increment of reinforcing materials induced by emergency brake of vehicles driving at a speed of 20 km/hr with that induced by vehicles driving at a constant speed of 20 km/hr is helpful in understanding the impact of driving conditions on the stresses developed in reinforcing materials. Shown in Fig. 12 is the monitoring result of the stress and force increments induced by emergency brake of a 12-ton truck driving through uphill and downhill conditions at a speed of 20 km/hr. In addition, monitoring results of the 12-ton truck driving at a constant speed of 20 km/hr through the uphill and downhill road conditions are also shown in Fig. 12.

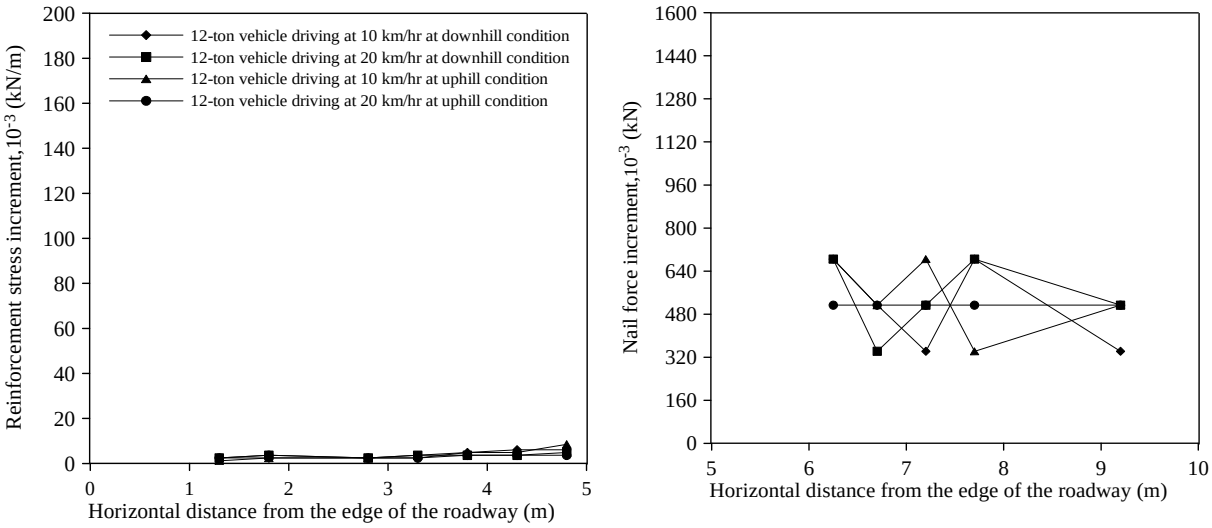

(a) depth = 4.5 m

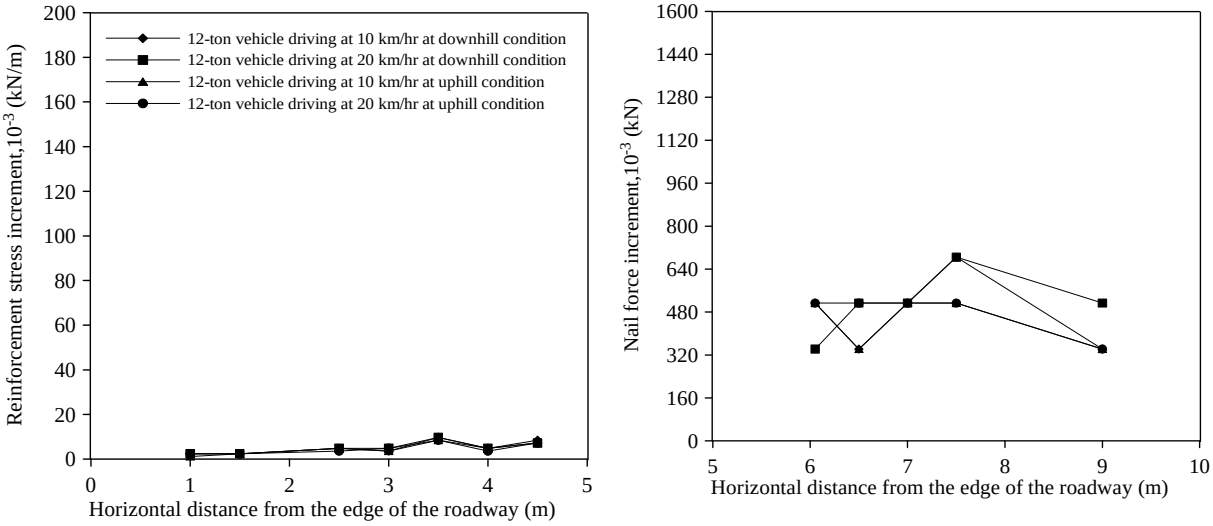

(b) depth = 3.5 m

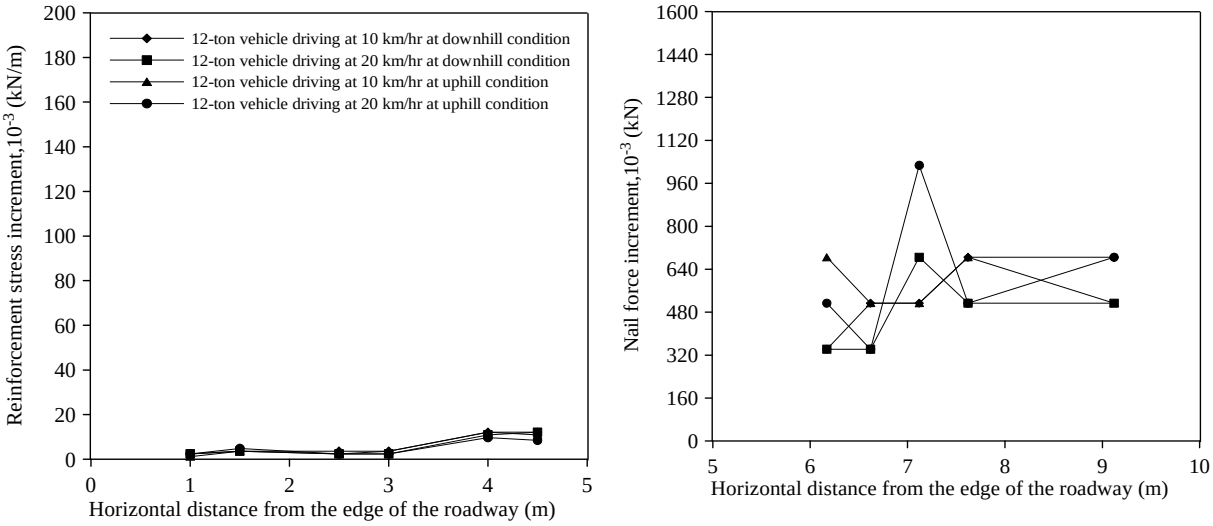

(c) depth = 2.5 m

Fig. 11 Reinforcement (geogrid) stress increment and nail force increment within the embankment subjected to 12-ton moving vehicle

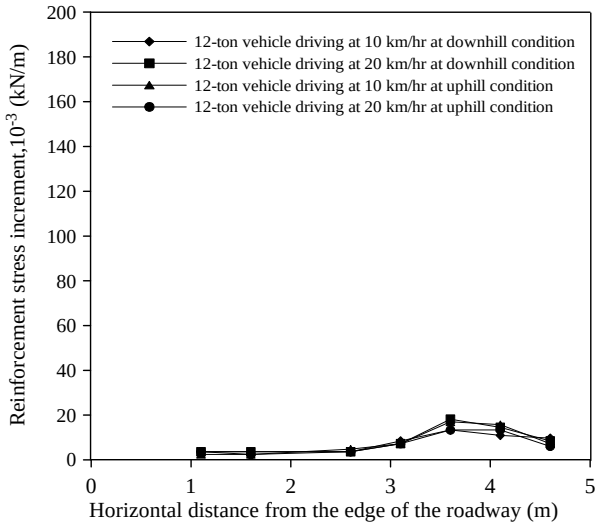

(d) depth = 2 m

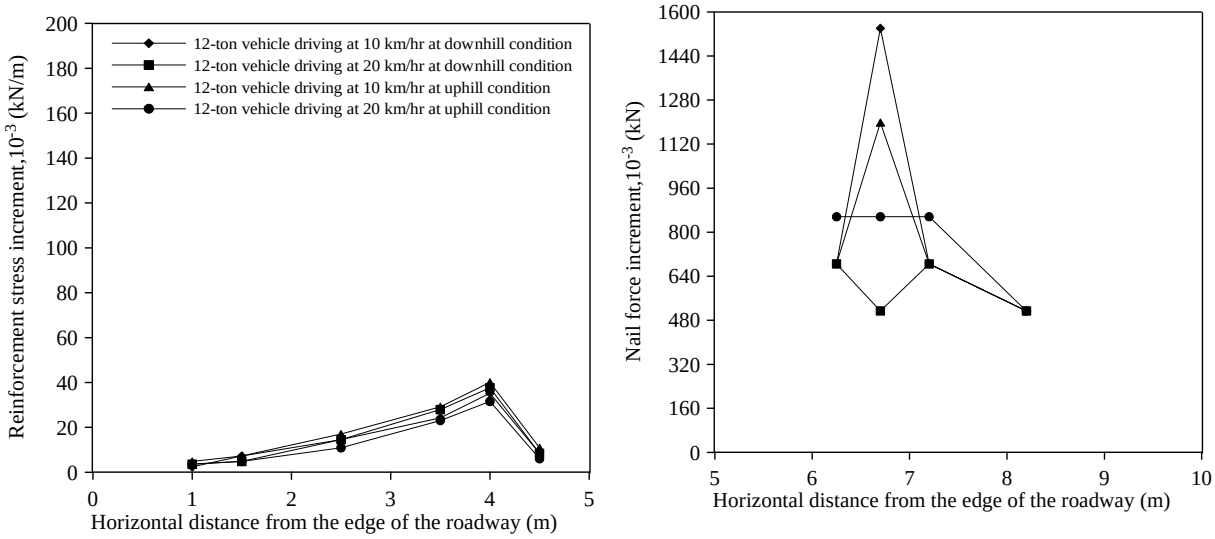

(e) depth = 1.5 m

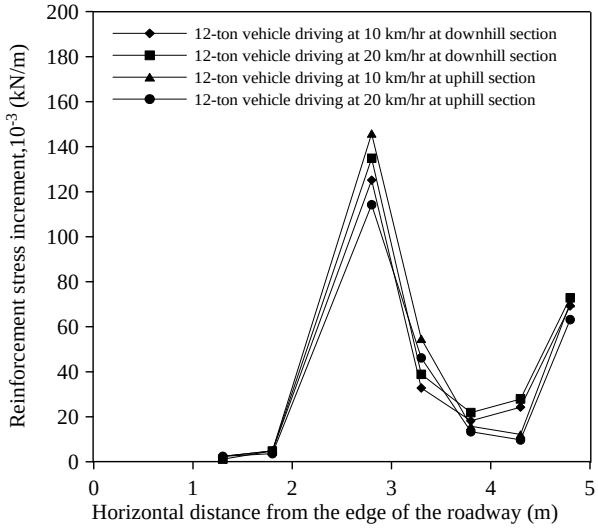

(f) depth = 1 m

Fig. 11 Reinforcement (geogrid) stress increment and nail force increment within the embankment subjected to 12-ton moving vehicle (continued)

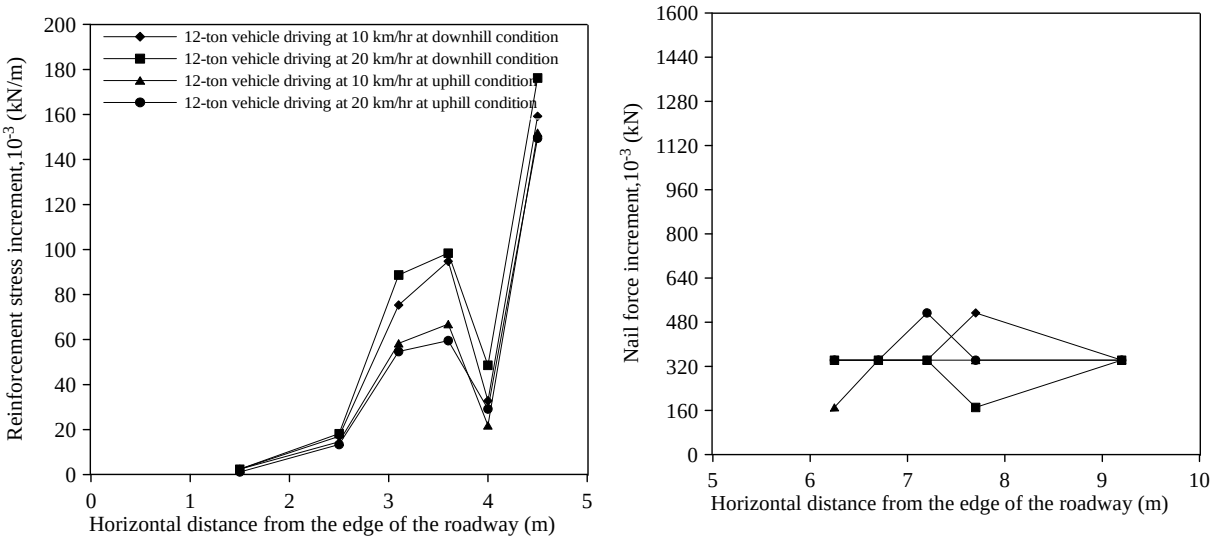

(g) depth = 0.5 m

Fig. 11 Reinforcement (geogrid) stress increment and nail force increment within the embankment subjected to 12-ton moving vehicle (continued)

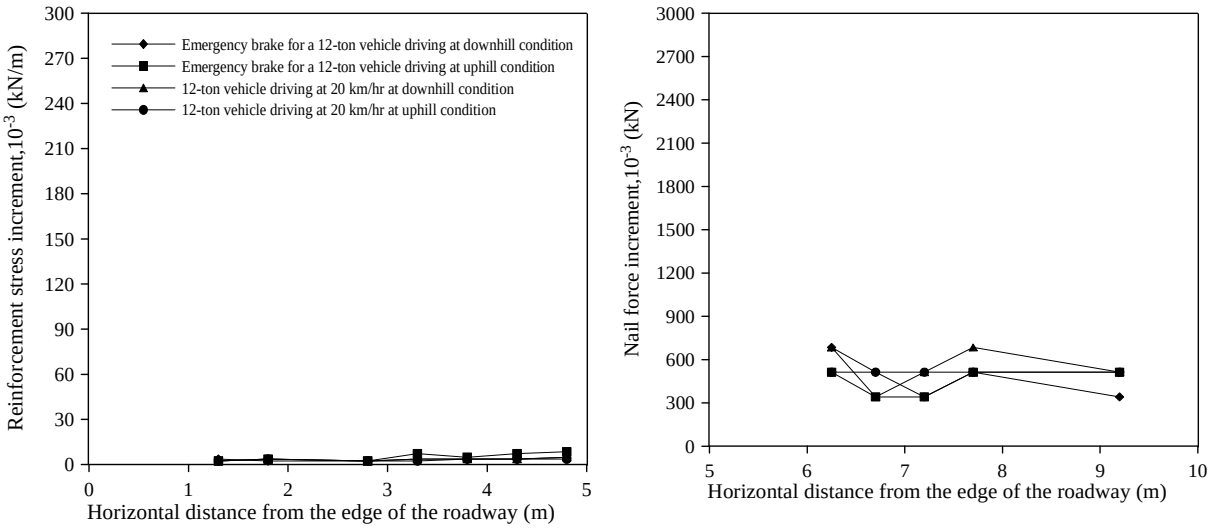

(a) depth = 4.5 m

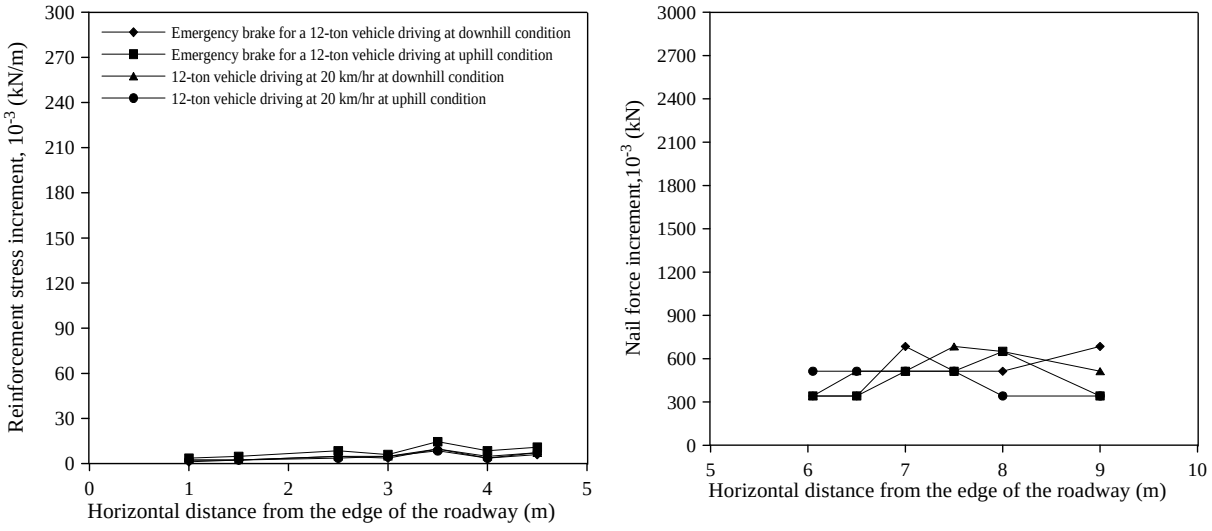

(b) depth = 3.5 m

Fig. 12 Reinforcement (geogrid) stress increment and nail force increment induced by braking of 12-ton vehicles driving at 20 km/hr

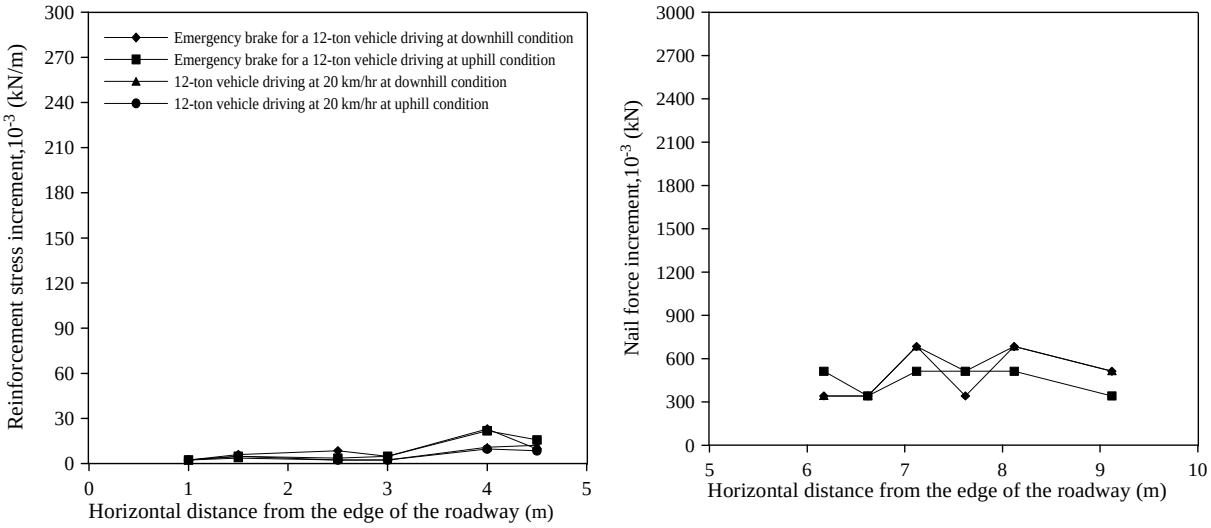

(c) depth = 2.5 m

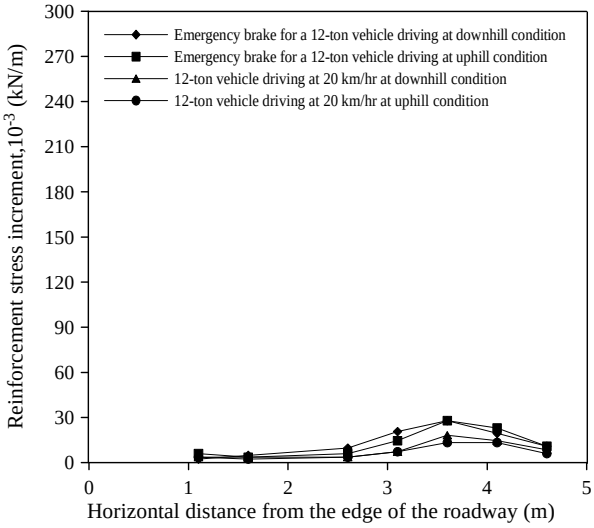

(d) depth = 2 m

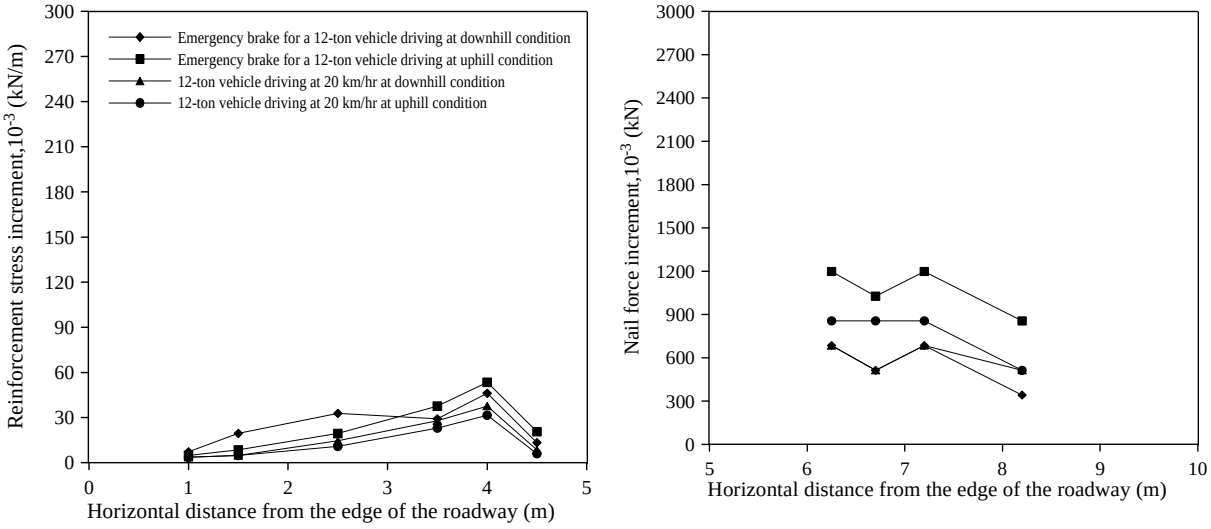

(e) depth = 1.5 m

Fig. 12 Reinforcement (geogrid) stress increment and nail force increment induced by braking of 12-ton vehicles driving at 20 km/hr (continued)

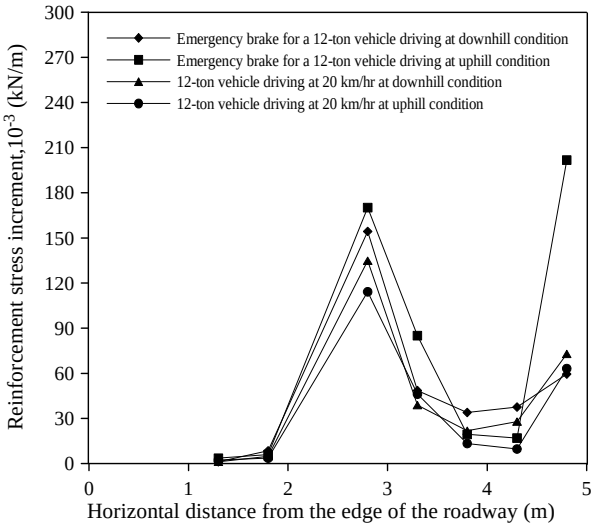

(f) depth = 1 m

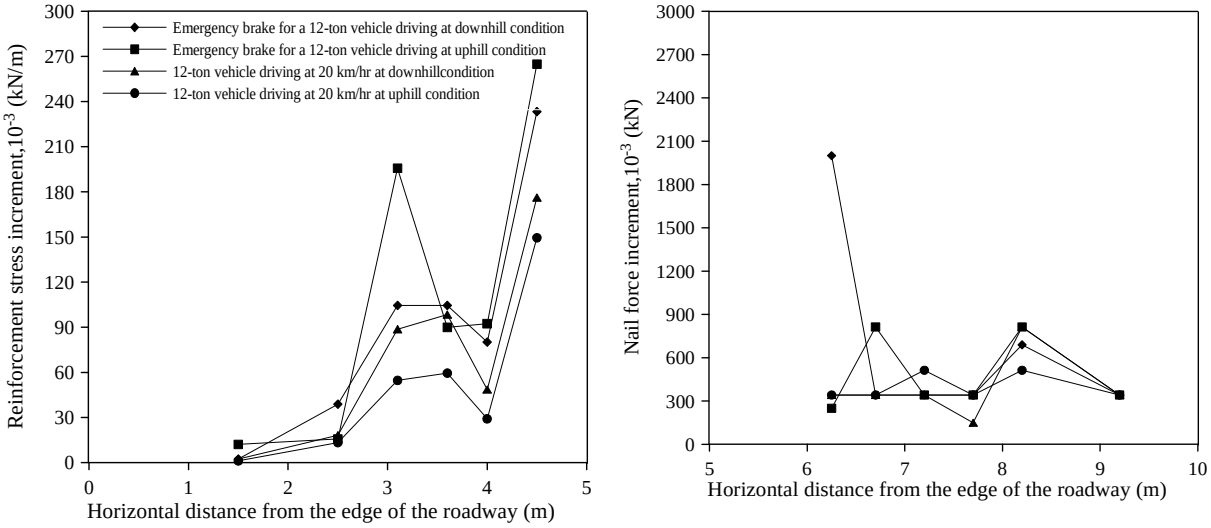

(g) depth = 0.5 m

Fig. 12 Reinforcement (geogrid) stress increment and nail force increment induced by braking of 12-ton vehicles driving at 20 km/hr (continued)

The tensile stress increment on reinforcements and soil nails caused by emergency brake of moving vehicles is higher than that induced by vehicles driving at a constant speed. In addition, the stress increment on reinforcements caused by emergency brake at uphill conditions is greater than that at downhill conditions. The reinforcement at shallow depths developed a greater tensile force increment while driving at uphill conditions and pressing the emergency brake comparing with the results at downhill conditions. Greater force increments on soil nails were mobilized within 1 m below the road surface at braking conditions. The maximum stress increment on reinforcements at 0.5 m and 1.0 m below the roadway under braking conditions occurred at the end section of the reinforcement, with a value of 0.27 kN/m and 0.21 kN/m, respectively. Following the completion of the construction of the embankment, the maximum tensile stress on the reinforcement at 1 m below the road surface was 3.6 kN/m, and the maximum tensile force increment on the reinforcement caused by braking was about 6% of that following the construction. For 12-ton truck driving through uphill conditions at a constant speed of 20 km/hr, the maximum tensile force increment on the reinforcement at 0.5 m below the road surface was about 0.15 kN/m. This value is about 55% of that induced at braking condition.

The tensile force increment caused by braking of vehicles during driving conditions at the front of the soil nails, *i.e.* near the connection between soil nails and reinforcements, was noticeably mobilized compared with that at the central and back portions. In addition, the force increment of soil nails induced by braking of the 12-ton truck at shallow depths is greater than that at greater depths. The maximum force increment of the soil nail at 0.5 m and 1.5 m below the road surface occurred at its front end, with a value of 2.1 kN and 1.2 kN, respectively. These values are greater than that induced by vehicles driving at a constant speed (20 km/hr). The maximum tensile force at 1.5 m below the road surface following the completion of the construction of the embankment was 22 kN. Therefore, the maximum force increment on the soil nail at 1.5 m below the road surface induced by braking of 12-ton vehicle was about 5.5% of that following the completion of the embankment.

4. CONCLUSIONS

This paper presents field monitoring results on the performance of an 8-m-high hybrid reinforced earth embankment built adjacent to a slope with narrow fill space. Reinforcement stresses and nail forces developed in the embankment system during the construction were investigated. In addition, reinforcement stresses and nail forces developed under static and traffic loadings were also investigated and discussed. Major findings summarized from this field monitoring project are: (1) The maximum reinforcement stress reaches to about 4 kN/m, corresponding to a tensile strain of about 0.33%, and occurs at a depth of 4.5 m below the ground surface following the construction of the embankment; (2) The maximum nail force occurs at the head at various elevations following the construction; (3) The maximum nail force behind the embankment is about 160 kN and occurs at a depth of 4.5 m following the construction; (4) The reinforcement stress increment induced by a 20 kPa static loads on the roadway is about 8.3% of that induced following the construction; (5) Most of the reinforcement stresses are developed during the backfilling stage. (6) The maximum reinforcement stress increment induced by 12-ton vehicle driving at the uphill condition is approximately 25% ~ 30% of that induced by 20 kPa static loading; (7) No significant variance between the tensile stress increment induced by vehicles driving at uphill conditions and that at downhill conditions is found in this study; (8) For 12-ton vehicle driving through uphill conditions at a constant speed of 20 km/hr, the maximum tensile force increment on the reinforcement at 0.5 m below the road surface is about 0.15 kN/m, and this value is about 55% of that induced at braking condition; (9) The maximum force increment on soil nails at 1.5 m below the road surface caused by the 12-ton vehicle driving at a constant speed of 20 km/hr is about 5% of the nail force developed following the construction of the embankment.

ACKNOWLEDGMENTS

This research work was sponsored by the Kaohsiung County Government. This support is gratefully acknowledged.

REFERENCES

Allen, T. M., Christopher, B. R., and Holtz, R. D. (1992). "Performance of a 12.6 m high geotextile wall in Seattle, Washington." *Proceedings of Geosynthetics Reinforced Soil Retaining Walls*, J.T.H. Wu, Editor, 81–100.

Bathurst, R. J., Walters, D., Vlachopoulos, N., Burgess P., and Allan, T. H. (2000). "Fullscale testing of geosynthetic reinforced walls," *Proc., GeoDenver 2000*, ASCE Special Publication.

Bathurst, Richard J., Blatz, James A., and Burger, Martin H. (2003). "Performance of instrumented large-scale unreinforced and reinforced embankments loaded by a strip footing to failure." *Canadian Geotechnical Journal*, **40**(6), 1067–1083.

Chou, N. N. S. and Fan, C.-C. (2004). *Structure for Fastening Soil Nails to Reinforced Soil Retaining Walls*. U.S. Patent No. US6742967B1.

Elias, V. B., Christopher, R., and Berg, R. R. (2001). *Mechanically Stabilized Earth Walls and Reinforced Soil Slopes Design and Construction Guidelines.* U.S. Department of Transportation, Federal Highway Administration, Publication No. FHWA-NHI-00-043.

Fan, C.-C. and Heish, C.-C. (2007). "A hybrid embankment system used in repairing collapsed roadway in mountainous area." *Proc., 16th Southeast Asia Geotechnical Conference*, Kuala Lumpur, Malaysia, 8–11.

Fishman, K. L., Desai, C. S., and Sogge, R. L. (1993). "Field behavior of instrumented geogrid soil reinforced wall." *Journal of Geotechnical Engineering*, ASCE, **119**(8), 1293–1307.

Karpurapu, R. and Bathurst, R. J. (1995). "Behaviour of geosynthetic reinforced soil retaining walls using the finite element method." *Computers and Geotechnics*, **17**, 279–299.

Simac, M. R., Christopher, B. R., and Bonczkiewiz, C. (1990). "Instrumented field performance of a 6 m geogrid soil wall." *Proc., 4th International Conference on Geotextiles, Geomembranes & Related Products*, The Hague, 53–59.